

$p6$ - Chiral Resonating Valence Bonds in the Kagomé Antiferromagnet

Sylvain Capponi¹, V. Ravi Chandra^{2,3}, Assa Auerbach², and Marvin Weinstein⁴

¹ *Laboratoire de Physique Théorique, Université de Toulouse and CNRS, UPS (IRSAMC), F-31062, Toulouse, France*

² *Physics Department, Technion, Haifa 32000, Israel*

³ *School of Physical Sciences, National Institute of Science Education and Research, Institute of Physics Campus, Bhubaneswar, 751005, India and*

⁴ *SLAC National Accelerator Laboratory, Stanford, CA 94025, USA.*

(Dated: June 29, 2021)

The Kagomé Heisenberg antiferromagnet is mapped onto an effective Hamiltonian on the star superlattice by Contractor Renormalization. Comparison of ground state energies on large lattices to Density Matrix Renormalization Group justifies truncation of effective interactions at range 3. Within our accuracy, magnetic and translational symmetries are not broken (i.e. a spin liquid ground state). However, we discover doublet spectral degeneracies which signal the onset of $p6$ - chirality symmetry breaking. This is understood by simple mean field analysis. Experimentally, the $p6$ chiral order parameter should split the optical phonon degeneracy near the zone center. Addition of weak next to nearest neighbor coupling is discussed^a.

PACS numbers: 75.10.Jm, 75.40.Mg

The antiferromagnetic Heisenberg model on the Kagomé lattice

$$\mathcal{H} = J \sum_{\langle ij \rangle} \mathbf{S}_i \cdot \mathbf{S}_j, \quad J > 0, \quad S = \frac{1}{2}, \quad (1)$$

is a much studied paradigm for frustrated quantum magnetism. In the classical approximation $S \rightarrow \infty$, this model exhibits macroscopic ground state degeneracy which encumbers semiclassical approximations. There is evidence, both numerical and experimental (in $\text{ZnCu}_3(\text{OH})_6\text{Cl}_2$ [1]), that quantum fluctuations lead to a paramagnetic “spin liquid” ground state [2].

Exact diagonalization studies (ED) [3], and ED in the variational dimer singlets subspace [4], have not approached the thermodynamic limit, due to severe computer memory limitations. Many methods have proposed paramagnetic ground states, including lattice symmetry breaking “valence bonds crystals” [5–8], algebraic spin liquids [9] and a time reversal symmetry breaking, chiral spin liquid [10].

To date, the lowest energy on long cylinders has been found by Density Matrix Renormalization Group DMRG [11, 12]. The DMRG ground state is a translationally invariant singlet, with apparently no broken translational or rotational symmetries. This state is consistent with a resonating valence bonds (RVB) state [13] with a spin gap $\Delta_{S=1} = 0.13$, (henceforth we express energies in units of J), and \mathbb{Z}_2 topological order [12, 14]. It is still unclear however, what are the low-energy singlet excitations of this state [11, 15], and whether or not any other symmetry of \mathcal{H} may be broken in the infinite two dimensional limit.

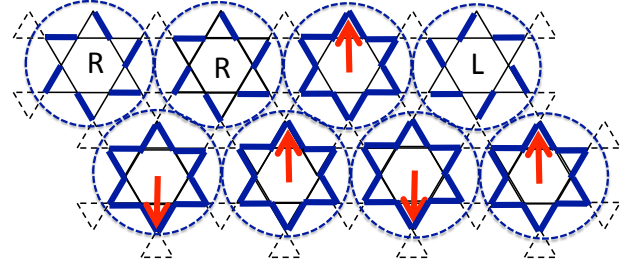


FIG. 1. The CORE-blocking scheme on the Kagomé lattice. R and L denote the two pinwheel ground states of the 12 site stars, and the arrows (pseudospins) denote the symmetrized Ising basis which spans the reduced Hilbert space of H^{CORE} , see Eq. (2).

This paper reports a surprising result: *The thermodynamic ground state appears to break reflection symmetries, and to possess two dimensional $p6$ chirality*, (– not to be confused with “spin chirality” which also breaks time reversal symmetry [10]). Our conclusion is obtained by Contractor Renormalization (CORE) [16] with 12-site stars blocking, see Fig. 1. the stars scheme is found to reach sufficient accuracy with range-3 interactions. This is evidenced by comparing ground state energies of the effective Hamiltonian H^{CORE_3} , to high precision DMRG on large lattices. The small modulation of bond energies is consistent, within our accuracy, with a translationally invariant singlet state as deduced by DMRG [11, 12].

H^{CORE_3} is diagonalized on up to 27 stars (effectively 324 Kagomé sites). The spectra exhibit doublet degeneracies between states with opposite parity under reflection [17]. These signal a hitherto unexpected spontaneous symmetry breaking in the thermodynamic limit into a chiral ground state. This chirality is understood as the effect of three-star interactions. Classical mean field

^a This work was supported by the U. S. DOE, Contract No. DE-AC02-76SF00515.

theory on the effective hamiltonian explains this symmetry breaking. A two-dimer chirality order parameter is defined on the microscopic Kagomé model. We propose an experimental signature of this broken symmetry in the phonon spectrum: a splitting of symmetry-protected degeneracy between two zone center optical modes [18].

Finally, we add weak ferromagnetic next nearest neighbor interactions J_2 , and find that it eliminates the chirality at $J_2 \approx -0.1$.

CORE procedure. Previous CORE calculations for the Kagomé model [19, 20] started with up-triangles blocking, and did not reach sufficient convergence at range 3. Here we use much larger and more symmetric blocks of 12 site (Magen David) stars which form a triangular superlattice. In each star, we retain just the two degenerate singlet ground states $|L_i\rangle$ and $|R_i\rangle$, depicted in Fig. 1 which form a pseudospin-1/2 basis:

$$\begin{aligned} |\uparrow_i\rangle &= \frac{1}{\sqrt{2+1/16}}(|R_i\rangle + |L_i\rangle), \\ |\downarrow_i\rangle &= \frac{1}{\sqrt{2-1/16}}(|R_i\rangle - |L_i\rangle). \end{aligned} \quad (2)$$

Note that the two states are C_6 -invariant, and have opposite parity under all D_6 reflections.

The CORE effective Hamiltonian on a superlattice of size N_s stars is defined by the cluster expansion,

$$\begin{aligned} H^{CORE} &= \sum_{i=1}^{N_s} h_i^{(1)} + \sum_{i_1 i_2} h_{i_1, i_2}^{(2)} + \dots + \sum_{i_1, \dots, i_{N_s}} h_{i_1, \dots, i_{N_s}}^{(N_s)}, \\ h_\alpha^{(n)} &\equiv H_\alpha^{(n)} - \sum_{m < n} \sum_{\beta(m) \in \alpha(n)} h_\beta^{(m)}. \end{aligned} \quad (3)$$

Here $\beta(m)$ is a connected subcluster of size m in a cluster $\alpha(n)$ of size n stars, and $h^{(n)}$ is defined to be an interaction of range- n . The operators $H_\alpha^{(n)}$ are constructed by ED of Eq. (1) on a Kagomé cluster α :

$$H_\alpha^{(n)} = \sum_\nu^{2^n} \epsilon_\nu^\alpha |\tilde{\Psi}_\nu^\alpha\rangle \langle \tilde{\Psi}_\nu^\alpha| \quad (4)$$

Here $(\epsilon_\nu^\alpha, \Psi_\nu^\alpha)$ are the exact 2^n lowest singlet energies and wavefunctions. The states $|\tilde{\Psi}_\nu^\alpha\rangle$ are an orthogonal basis constructed by sequential projections of $|\Psi_\nu^\alpha\rangle$, $\nu = 1, 2, \dots, 2^n$ onto the pseudospin states. After projection, the states are orthogonalized sequentially by using the Gram-Schmidt procedure.

If interactions of all ranges $n \leq N_s$ are included, then H^{CORE} has the identical low energy singlet spectrum as Eq. (1) on the equivalent Kagomé lattice. However, ED cost to compute $h^{(n)}$ grows exponentially with n . Thus, the success of CORE depends on the ability to truncate the cluster expansion at feasible n while maintaining sufficient accuracy in the truncated Hamiltonian.

The error in the ground state energy $\delta E_0^{CORE_n}$ can be computed by comparison to high-precision DMRG on large lattices with $m > n$ stars. This error should

	c_0	h	J^x	J^y	J^z
ED	-6.26391	0.13818	0.00713	-0.00105	-0.00045
PT	-5.268	0.046	0	-0.00025	-0.00175

TABLE I. Parameters of CORE range-2 Hamiltonian, by Exact Diagonalization, and second order Perturbation Theory [22].

be much smaller than the important interactions in H^{CORE_n} .

Lattice translations. Our choice of stars for the reduced Hilbert space *nominally* breaks lattice translational symmetry as seen in Fig. 1. The microscopic spin correlations are computed by functional differentiation of the CORE ground state energy with respect to source terms [21]. In principle one must compute the effective interactions to all ranges to restore full translational symmetry. Nevertheless, symmetry breaking artifacts decrease with the truncation range n . We can therefore identify any spontaneous translational symmetry breaking which significantly exceeds the truncation error.

CORE range 2. We start with the lowest-order truncation at range 2. The general form of the two-star interactions allowed by lattice reflection symmetries is

$$H^{CORE_2} = Nc_0 + h \sum_i \sigma_i^z + \sum_{\langle ij \rangle} J^\alpha \sigma_i^\alpha \sigma_j^\alpha, \quad (5)$$

where i labels sites, $\langle ij \rangle$ nearest neighbor bonds on the triangular lattice. σ^α , $\alpha = x, y, z$ are Pauli matrices.

The parameters derived from the lowest 4 eigenstates of 24 spins, are computed by Lanczos algorithm, and listed in Table I. It is instructive to compare the ED parameters to the second order perturbation theory (PT) in the inter-star bonds, as was calculated by Syromyatnikov and Maleyev citeSM. Second order PT in the connecting bonds is not very accurate when connecting bonds have exchanges equal to 1. For example, PT misses the important J^x interactions. The dominant interaction of H^{CORE_2} is the field $h = 0.138$, which would yield in the thermodynamic system a ferromagnetic ground state polarized in the $|\downarrow\rangle$ direction. In terms of Kagomé spins, the ground state would be a product of *antisymmetric* superposition of pinwheel states, with local \uparrow fluctuations generated by the xx, yy terms.

Within $CORE_2$, the connecting bonds energy is $E_{inter} = -0.21283$, versus the intra-star bonds at $E_{intra} = -0.2225$. Interestingly, the modulation is already diminished from 100% \rightarrow 4.3% with range-2 interactions.

How accurate is H^{CORE_2} ? Unfortunately, not enough. The exact ground state energy/site of \mathcal{H} for 36 sites is $E_0^{ED} = -0.41276$ while the $CORE_2$ energy/site for three stars is $E_0^{CORE_2} = -0.4277$. The error of -0.0149 is quite large relative to the important terms in H^{CORE_2} .

J_2	$J_2 = 0$ (Kagomé)	$J_2 = +0.1$	$J_2 = -0.1$
c_0	-5.24629	-5.17068	-5.48631
h	-0.069224	0.059323	-0.362797
J_x	-0.009028	-0.015421	0.001123
J_y	-0.011879	0.001832	-0.017699
J_z	0.021056	0.003686	0.020141
J_{zxx}	-0.027920	-0.019649	-0.009524
J_{zyy}	0.004550	-0.004749	0.002394
J_{zzz}	0.000660	-0.001410	0.010495

TABLE II. Interaction parameters of CORE range 3, with three values of J_2 .

Hence we cannot trust the truncation, and longer range interactions are needed.

CORE range 3. To obtain H^{CORE_3} we compute the interactions $h^{(3)}$ on the three star triangular cluster [23]. This required ED of Eq. (1) of 36 spins with open boundary conditions (OBC). For verification, we ran both a standard Lanczos routine on a supercomputer, and the memory-economical Lanczos-SVD routine [24] on a desktop computer. Adding contributions from ranges 1–3 we obtain the following effective hamiltonian

$$H^{CORE_3} = Nc_0 + \sum_i h\sigma_i^z + \sum_{\langle ij \rangle, \alpha} J_\alpha \sigma_i^\alpha \sigma_j^\alpha + \sum_{\langle ijk \rangle_\Delta, \alpha} J_{z\alpha\alpha} \sigma_i^z \sigma_j^\alpha \sigma_k^\alpha, \quad (6)$$

where $\langle ijk \rangle_\Delta$ label nearest neighbor triangles on the triangular lattice. We do not list terms that cancel in the superlattice summation with Periodic Boundary Conditions (PBC).

The H^{CORE_3} truncation error is estimated by comparing its ground state energy on clusters of sizes $N > 3$ to high precision DMRG [25, 26]. From Table III we find that the truncation error is very satisfactory < 0.004 per site. If we extrapolated $CORE_3$ ground state energy to the thermodynamic limit, we get -0.447 which underestimates the extrapolated DMRG result -0.439 [12] by at most -0.008 per site. We see in Table II for comparison, that the values of the dominant terms h , J_{zxx} and J_z (multiplied by number of bonds/site), are significantly larger than this error. *Thus, we believe that CORE truncation at range 3 is sufficiently accurate to obtain the correct thermodynamic phase.*

p6-Chirality. The ED spectrum of H^{CORE_3} is evaluated on lattices of up to $N_s = 27$ stars (324 Kagomé sites), with PBC. The most striking feature on lattices larger than $N_s = 9$, is the emergence of ground state degeneracy of two singlets with opposite parity under reflections. In the pseudospin representation, even (odd) parity states include only an even (odd) number of stars with antisymmetric $|\downarrow\rangle$ states. These degeneracies signal a spontaneous reflection symmetry breaking $p6m \rightarrow p6$

number of stars	$E_0^{CORE_3}$	E_0^{DMRG}	Error
2×2	-0.418452	-0.417213	-0.001239
2×3	-0.423953	-0.422336	-0.001617
3×4	-0.431150	-0.428046	-0.003104
3×5	-0.432688	-0.429191	-0.003497

TABLE III. Ground state energies per site of H^{CORE_3} , and comparison to DMRG on equivalent Kagomé clusters (with OBC).

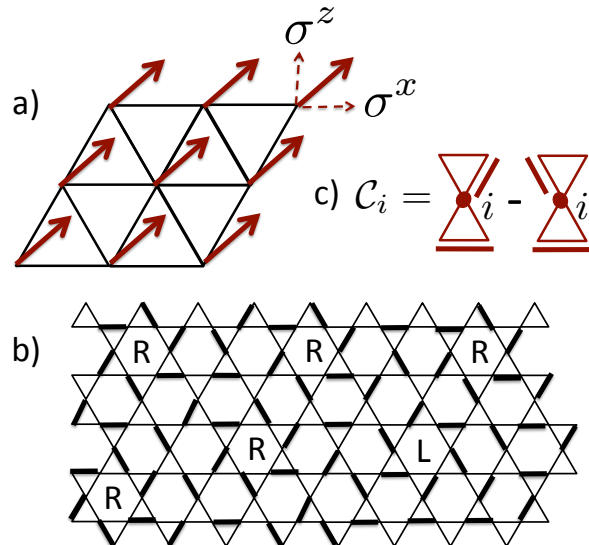


FIG. 2. a) The mean field ground state of H^{CORE_3} exhibiting $\langle \sigma^x \rangle > 0$ order, which corresponds to two dimensional chirality. b) A typical singlets configuration in the corresponding ground state of the Kagomé lattice. Notice that there is no translational order, but that there are more pinwheel configurations of $|R\rangle$ than $|L\rangle$. c) The two dimer chiral order parameter defined in Eq.8.

in the thermodynamic limit.

A Mean Field (MF) energy of H^{CORE_3} in spin-1/2 coherent states $|\Omega_i\rangle$ is

$$E^{MF} = Nc_0 + h \sum_i \cos \theta_i + \sum_{\langle ij \rangle, \alpha} J_\alpha \Omega_i^\alpha \Omega_j^\alpha + \sum_{\langle ijk \rangle, \alpha} J_{z\alpha\alpha} \cos \theta_i \Omega_j^\alpha \Omega_k^\alpha, \quad (7)$$

where $\Omega_i = (\sin \theta_i \cos \phi_i, \sin \theta_i \sin \phi_i, \cos \theta_i)$. In Table II we see that for $J_2 = 0$, the dominant couplings are the

J_2	M_z^{MF}	M_z^{ED}
0.0	0.2647	0.2257
+0.1	0.1390	0.1476
-0.1	0.5	0.4999

TABLE IV. Effect of next nearest neighbor couplings on the ground state z -polarization.

field h , and the J_z and J_{zxx} exchanges. The last coupling is responsible for the chiral symmetry breaking, as it pulls the spins in the $\pm\hat{x}$ direction.

Minimizing E^{MF} , we find a ferromagnetic state depicted in Fig. 2(a). The z -polarization $M_z^{MF} = \frac{1}{2} \cos\bar{\theta}$ is compared to ED in Table IV. For $J_2 = 0$, we find that the chirality order is substantial with $\frac{1}{2} \sin\bar{\theta} = 0.424$ by MF, and $\frac{1}{2} \langle \sigma^x \rangle = 0.397$ by ED.

In Fig. 2(b) we depict a typical dimer configuration which contributes to the $p6$ - chiral RVB state. One can see the predominance of R pinwheel chirality over L . The most local order parameter for this chirality is the two dimer correlation depicted in Fig. 2(c),

$$C_i = \sum_{\mathbf{d}} (\mathcal{S}_{\mathbf{d}} \mathcal{S}_{\eta^r(\mathbf{d})} - \mathcal{S}_{\mathbf{d}} \mathcal{S}_{\eta^l(\mathbf{d})}), \quad (8)$$

where the dimer singlet projectors are

$$\mathcal{S}_{\mathbf{d}} = 1/4 - \mathbf{S}_{\mathbf{d}_1} \cdot \mathbf{S}_{\mathbf{d}_2}, \quad (9)$$

and $\eta^r(\mathbf{d})$ ($\eta^l(\mathbf{d})$) is the bond emanating from i at angle $\pi/3$ ($2\pi/3$) relative to the dimer bond opposing i . The two terms in \mathcal{C} measure parts of pinwheels of opposite chirality.

Translational symmetry. At range 3, the energy of internal triangles $E_{\Delta_{inter}} = -0.686$, and connecting triangles is $E_{\Delta_{intra}} = -0.665$ (depicted by solid and dashed lines respectively in Fig. 1). This relative modulation of about 3.0% lies within the truncation error. Thus we can affirm that CORE_3 ground state is consistent with *translational invariance* in agreement with DMRG [11, 12].

Singlet Excitations. In the 27 star lattice, the lowest singlet excitation above the two degenerate ground states is $\Delta E_{S=0} = 0.28$, which has a non zero wavevector. This excitation gap does not vary much with lattice size. Within the pseudospin Hamiltonian, it can be understood as a local spin flip from the ferromagnetic ground state. We note that the singlet gap is slightly higher than two $S = 1$ magnons at energies $E_{S=1} = 0.13$. This conclusion differs from that obtained by ED on 36 site PBC, which found a large number of singlets below the spin gap [27]. Since our effective Hamiltonian describes excitations on much larger lattices, we are inclined to associate these low singlets with the smaller PBC lattice geometry.

Experimentally, fluctuating two-dimer correlations are tricky to observe directly. Fortunately, real compounds have sizable magneto-elastic coupling between the ions and the dimer singlets. While, on average, dimer density and bond lengths are uniform in the RVB state, *dimer density fluctuations*, $\delta\rho_d$ governed by the characteristic singlet energy scale, are linearly coupled to the ionic displacements. In Fig. 3, the effect of a temporary excess of dimers on a triangle is shown. In the chiral phase, imbalance between the left and right bonds emanating out of the triangle produces a chiral force on the ions as

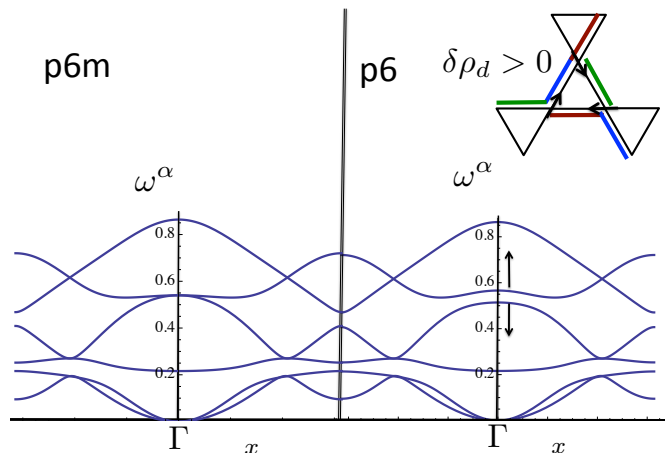


FIG. 3. Kagomé phonon spectra in $p6m$ phase, and $p6$ - chiral phase, calculated within a nearest neighbor spring constant model given in Ref.[28]. In the top right, the dimer chiral correlations induce a linear coupling between excess dimer density $\delta\rho_d$ and chiral ionic displacements, as depicted by the arrows. This adds a chiral term to the dynamical matrix which splits the degeneracy of the optical phonons at the zone center.

depicted by the arrows. Integrating out the dimer density fluctuations results in a chiral perturbation to the phonon dynamical matrix [17]. By symmetry [18], the degeneracy between two optical modes is removed at the zone center, as shown in Fig. 3.

Finite J_2 . We have added next nearest neighbor interactions with coupling J_2 to Eq. (1), and calculated the parameters of H^{CORE_3} , as shown in Table II. For $J_2 = 0.1$, we find the same doublet degeneracies, and chirality, as for the pure model $J_2 = 0$ [14]. In contrast, for a weak negative $J_2 = -0.1$ the spectrum changes dramatically: The doublets are removed, and the ground state is fully polarized in the \uparrow direction. The precise nature of this phase has not been yet explored. Interestingly, we notice that in proximity to the parameters of Table II, one finds the Ising antiferromagnet in field. Its ground state contains ferromagnetic hexagons with reversed spins in their center. It represents the Hexagonal Valence Bond Solid state, previously shown to have low variational energies [5], and proposed for $J_2 \simeq -0.1$ [29].

Summary. Using CORE we arrived at an effective Hamiltonian, whose accuracy was determined to be sufficiently high so as to trust its predictions for the thermodynamic limit. Its ground state is consistent with a translationally invariant RVB phase, but with broken $p6$ chiral symmetry. A 2-dimer chiral order parameter is defined, which may be numerically explored on large lattices. Experimentally, it may be detected by splitting of optical phonon degeneracy.

Acknowledgements. We thank Andreas Läuchli, Daniel Podolsky and Didier Poilblanc, for useful discussions. AA and SC acknowledge the hospitality of the Aspen

Center for Physics and KITP at Santa Barbara, supported by the NSF Grants PHY-1066293 and PHY-1125915. Funding from U. S. DOE, Contract No. DE-AC02-76SF00515, Israel Science Foundation and U.S. – Israel Binational Science Foundation are acknowledged. Numerical simulations were performed at CALMIP.

-
- [1] Oren Ofer *et al.*, (unpublished) arXiv:cond-mat/0610540; J. S. Helton *et al.*, Phys. Rev. Lett. **98**, 107204 (2007). A. Olariu, *et al.*, Phys. Rev. Lett. **100**, 087202 (2008); K. Matan *et al.*, Phys. Rev. B **83**, 214406 (2011).
- [2] L. Balents, Nature (London) **464**, 199 (2010).
- [3] C. Zeng and V. Elser, Phys. Rev. B **42**, 8436 (1990); P. Lecheminant, B. Bernu, C. Lhuillier, L. Pierre, and P. Sindzingre, Phys. Rev. B **56**, 2521 (1997); C. Waldtmann, H.-U. Everts, B. Bernu, C. Lhuillier, P. Sindzingre, P. Lecheminant, and L. Pierre, Eur. Phys. J. B **2**, 501 (1998); H. Nakano and T. Sakai, Jour. Phys. Soc. Japan, **80**, 53704 (2011); A. M. Läuchli, J. Sudan, and E. S. Sørensen, Phys. Rev. B **83**, 212401 (2011). Recently, 48 spins have been diagonalized (A. M. Läuchli, private communication).
- [4] C. Zeng and V. Elser, Phys. Rev. B **51**, 8318 (1995); M. Mambrini and F. Mila, Eur. Phys. J. B **17**, 651 (2000).
- [5] J. B. Marston and C. Zeng, J. Appl. Phys. **69**, 5962 (1991); P. Nikolic and T. Senthil, Phys. Rev. B **68**, 214415 (2003); R. R. P. Singh and D. A. Huse, Phys. Rev. B **77**, 144415 (2008).
- [6] G. Evenbly and G. Vidal, Phys. Rev. Lett. **104**, 187203 (2010).
- [7] D. Poilblanc, M. Mambrini, D. Schwandt, Phys. Rev. B **81**, 180402(R) (2010); D. Poilblanc and G. Misguich, Phys. Rev. B **84**, 214401 (2011).
- [8] B. Clark, J. Kinder, E. Neuscamman, G. K.-L. Chan, M. J. Lawler, arXiv:1210.1585, unpublished.
- [9] M. Hermele, Y. Ran, P. A. Lee, and X. G. Wen, Phys. Rev. B **77**, 224413 (2008); Y. Iqbal, F. Becca, and D. Poilblanc, Phys. Rev. B **84**, 020407 (2011).
- [10] L. Messio, B. Bernu, and C. Lhuillier, Phys. Rev. Lett. **108**, 207204 (2012).
- [11] S. Yan, D. A. Huse, and S. R. White, Science **332**, 1173 (2011).
- [12] S. Depenbrock, I. P. McCulloch, and U. Schollwöck, Phys. Rev. Lett. **109**, 067201 (2012).
- [13] P. Fazekas and P. W. Anderson, Philos. Mag. **30**, 423 (1974).
- [14] H.-C. Jiang, Z. Wang, and L. Balents, arXiv:1205.4289.
- [15] H. C. Jiang, Z.Y. Weng, and D. N. Sheng, Phys. Rev. Lett. **101**, 117203 (2008).
- [16] C. J. Morningstar, M. Weinstein Phys. Rev. D **54**, 4131 (1996); M. Weinstein, Phys. Rev. B **63**, 174421 (2001); M. S. Siu and M. Weinstein Phys. Rev. B **77**, 155116 (2008).
- [17] Supplementary material.
- [18] We are indebted to Daniel Podolsky for suggesting to us this idea.
- [19] R. Budnik and A. Auerbach Phys. Rev. Lett. **93**, 187205 (2004).
- [20] S. Capponi, A. Läuchli, and M. Mambrini Phys. Rev. B **70**, 104424 (2004).
- [21] E. Altman and A. Auerbach, Phys. Rev. B **65**, 104508 (2002); E. Berg, E. Altman, and A. Auerbach, Phys. Rev. Lett. **90**, 147204 (2003).
- [22] A. V. Syromyatnikov and S. V. Maleyev, Phys. Rev. B **66**, 132408 (2002); A. V. Syromyatnikov and S. V. Maleyev, JETP **98**, 538 (2004).
- [23] We order the clusters in terms of their radii. Thus three star lines are considered longer range than the triangle. Three star 120° are not included in the cluster expansion, as they get cancelled in embedding range 4 rhombi [21], and E. Altman, Ph.D. thesis, Technion, unpublished.
- [24] M. Weinstein, A. Auerbach, and V. R. Chandra, Phys. Rev. E **84**, 056701 (2011).
- [25] S. R. White, Phys. Rev. Lett. **69**, 2863 (1992).
- [26] We use open boundary conditions on these clusters, and keep up to to get a discarded weight smaller than 10^{-5} . Note that these variational DMRG energies give exact upper bounds on the ground-state energy [11].
- [27] P. Sindzingre, C. Lhuillier, Europhys. Lett. **88**, 27009 (2009).
- [28] L. Zhang, J. Ren, J.-S. Wang and B. Li, J. Phys.: Condens. Matter **23**, 305402 (2011).
- [29] O. Ma and J. B. Marston, Phys. Rev. Lett. **101**, 027204 (2008); Y. Iqbal, F. Becca, and D. Poilblanc, Phys. Rev. B **83**, 100404(R) (2011).

Supplement: p6-Chiral Resonating Valence Bonds in the Kagomé Antiferromagnet

Sylvain Capponi¹, V. Ravi Chandra^{2,3}, Assa Auerbach³, and Marvin Weinstein⁴

¹ *Laboratoire de Physique Théorique, Université de Toulouse and CNRS, UPS (IRSAMC), F-31062, Toulouse, France*

² *Physics Department, Technion, Haifa 32000, Israel*

³ *National Institute of Science Education and Research (NISER), IOP Campus, Bhubaneswar, 751005, India and*

⁴ *SLAC National Accelerator Laboratory, Stanford, CA 94025, USA.*

(Dated: June 29, 2021)

Here we provide details of the exact diagonalization of H^{CORE_3} on 27 stars, and the effects of the chiral order parameter on the optical phonons of the Kagomé ions.

EXACT DIAGONALIZATION OF 27 STARS

In Fig. 1 we plot the exact spectrum of 27 stars with periodic boundary conditions. Since this cluster has all translations and the full C_{6v} point group symmetry, we can label eigenstates according to their symmetry quantum numbers. The 6 inequivalent momenta are shown in the plot, and for each of them, we can make use of the little group, i.e. the reduced symmetry group that leaves the momentum invariant: at Γ point, the little group is C_{6v} , at K point C_{3v} , while A, B, C, and D momenta only have a single Z_2 reflection. Therefore, we can label few low-energy states according to the irreducible representations of these groups.

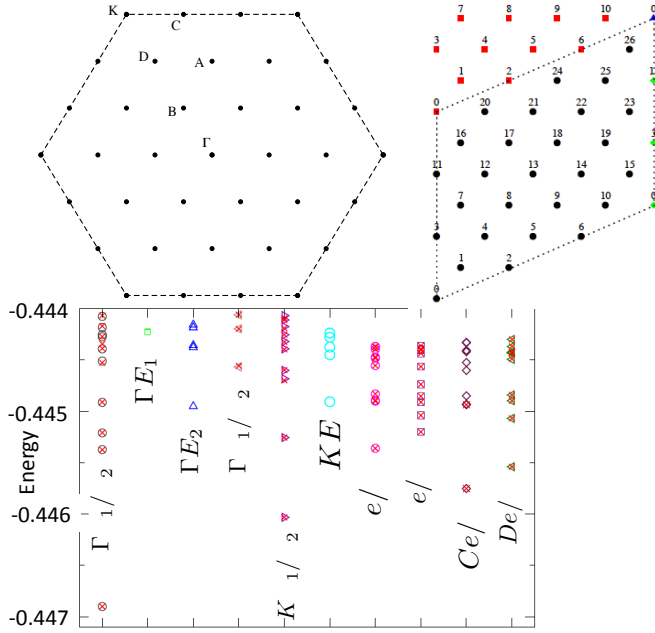


FIG. 1. Top: a cluster of 27 sites on the triangular superlattice, and its wavevectors in the Brillouin Zone Spectrum. Bottom: The singlet spectrum of H^{CORE_3} on this cluster (equivalent to 324 Kagomé spins). Notice the nearly exact doublet degeneracies, including the ground state doublet at $\Gamma A_1, \Gamma A_2$. These degeneracies signal $p6m \rightarrow p6$ spontaneous symmetry breaking in the thermodynamic limit.

COUPLING OF THE CHIRAL ORDER PARAMETER AND THE PHONON SPECTRUM

$p6m$ Model

A simple model for the phonon spectrum of the planar Kagomé was worked out by L. Zhang *et al.* in Ref. [1]. The two dimensional ionic displacements \mathbf{u}_i are labelled by $i=1=$ bottom left, $2=$ bottom right, and $3=$ top site. The nearest neighbor force constant matrix in the xy basis is

$$K_x = \begin{pmatrix} K_L & 0 \\ 0 & K_T \end{pmatrix} \quad (1)$$

where we K_L and K_T are longitudinal and transverse force constants respectively. We follow Ref. [1] and take $K_T = K_L/4$. A rotation is defined:

$$U = \begin{pmatrix} \cos(\pi/3) & -\sin(\pi/3) \\ \sin(\pi/3) & \cos(\pi/3) \end{pmatrix} \quad (2)$$

with which we express the rotated force constant matrices

$$K_{12} = K_x, \quad K_{13} = UK_x U^\dagger, \quad K_{23} = U^\dagger K_x U \quad (3)$$

These matrices define blocks in the 6×6 spring constant matrices

$$\begin{aligned} K_0 &= \begin{pmatrix} 2(K_{12} + K_{13}) & -K_{12} & -K_{13} \\ -K_{12} & 2(K_{12} + K_{23}) & -K_{23} \\ -K_{13} & -K_{23} & 2(K_{13} + K_{23}) \end{pmatrix} \\ K_1 &= \begin{pmatrix} 0 & 0 & 0 \\ -K_{12} & 0 & 0 \\ 0 & 0 & 0 \end{pmatrix} & K_2 &= \begin{pmatrix} 0 & 0 & 0 \\ 0 & 0 & 0 \\ -K_{13} & 0 & 0 \end{pmatrix} \\ K_3 &= \begin{pmatrix} 0 & 0 & 0 \\ 0 & 0 & 0 \\ 0 & -K_{23} & 0 \end{pmatrix} & K_4 &= \begin{pmatrix} 0 & -K_{12} & 0 \\ 0 & 0 & 0 \\ 0 & 0 & 0 \end{pmatrix} \\ K_5 &= \begin{pmatrix} 0 & 0 & -K_{13} \\ 0 & 0 & 0 \\ 0 & 0 & 0 \end{pmatrix} & K_6 &= \begin{pmatrix} 0 & 0 & 0 \\ 0 & 0 & -K_{23} \\ 0 & 0 & 0 \end{pmatrix} \end{aligned} \quad (4)$$

The dynamical matrix in \mathbf{q} -space is

$$\begin{aligned} K(\mathbf{q}) &= K_0 + K_1 e^{iq_x} + K_2 e^{i(\frac{q_x}{2} + \frac{\sqrt{3}q_y}{2})} \\ &+ K_3 e^{i(-\frac{q_x}{2} + \frac{\sqrt{3}q_y}{2})} + K_4 e^{-iq_x} \\ &+ K_5 e^{i(-\frac{q_x}{2} - \frac{\sqrt{3}q_y}{2})} + K_6 e^{i(\frac{q_x}{2} - \frac{\sqrt{3}q_y}{2})} \end{aligned} \quad (5)$$

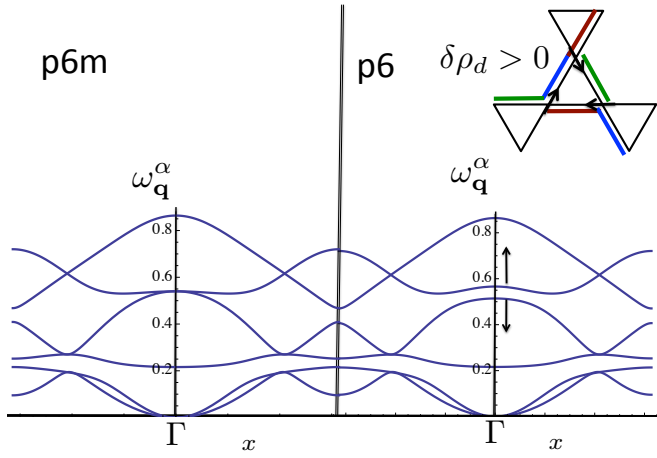


FIG. 2. Kagomé phonon spectra in p6m and p6-Chiral phases, calculated within a nearest neighbor spring constant model given in Ref. [1]. In the top right, the dimer chiral correlations induce a linear coupling between excess dimer density and chiral ionic displacements, as depicted by the arrows. This adds a chiral term to the dynamical matrix and splits the degeneracy of the optical phonons at the zone center.

Chiral Symmetry Breaking RVB – A magneto-elastic coupling $\frac{\delta J}{\delta u}$ exerts a force on the atoms on either side of a singlet dimer toward each other. However, the RVB phase has a uniform average density of dimers on all bonds. There are however dynamical fluctuations of the dimer density which can be modelled by a harmonic Lagrangian

$$\mathcal{L}_d = \frac{1}{2} \int d^2x \frac{1}{2} (\partial_t^2 - \omega_d^2) \delta \rho_d^2(\mathbf{x}) \quad (6)$$

where ω_d is of the order of the singlet excitation energies.

Let us consider a RVB phase with positive chirality given by $\langle \mathcal{C} \rangle > 0$. An instantaneous excess dimer density on the up-triangle is shown in Fig. 2. (In any dimer covering, some fraction of the triangles have no dimers, and thus lower than the average density). Due to right chirality, the neighboring triangles' dimers directions are biased to emanate rightward relative to the opposite edge. As a consequence, each corner of our triangle feels a net "pull" along the direction of its (on the average) uncompensated bond. This amounts to an effective coupling

$$\mathcal{L}_{d-ion} = -\gamma |\langle \mathcal{C} \rangle| \int d^2x \delta \rho_d^2(\mathbf{x}) \mathbf{v}^r \cdot \mathbf{u}(\mathbf{x}) \quad (7)$$

where \mathbf{u} is the ion displacements vector, and \mathbf{v}^r is given as the 6-dimensional clockwise displacements,

$$\mathbf{v}^r = \frac{1}{\sqrt{3}} (\cos(\frac{\pi}{3}), \sin(\frac{\pi}{3}), -1, 0, \cos(\frac{\pi}{3}), -\sin(\frac{\pi}{3}))$$

By integrating out the gapped dimer density fluctuations, a chiral correction to the quadratic dynamical matrix is obtained

$$D^{chiral}(\mathbf{q}) = D(\mathbf{q}) - \frac{\gamma^2 |\langle \mathcal{C} \rangle|^2}{\omega_d} \mathbf{v}^r \mathbf{v}^r \quad (8)$$

This correction lifts the degeneracy of the optical phonons at $\mathbf{q} = 0$ as shown in Fig. 2.

[1] L. Zhang, J. Ren, J.-S. Wang and B. Li, J. Phys.: Condens. Matter **23**, 305402 (2011). There is a typographical error in the labeling of the K_i matrices was corrected here.